Preparation of Biocompatible Aggregation-Induced Emission Homopolymeric Nanoparticles for Cell Imaging[a]

Chunping Ma, Qingqing Ling, Shidang Xu, Hongni Zhu, Ge Zhang,* Xie Zhou, Zhenguo Chi,* Siwei Liu, Yi Zhang, Jiarui Xu*

A series of new homopolymers with various degrees of polymerization derived from vinyl tetraphenylethene, that is, poly[2-(4-vinylphenyl)ethene-1,1,2-triyl)tribenzene] homopolymers, is synthesized by reversible addition–fragmentation chain transfer (RAFT) polymerization. The homopolymers exhibit a significant aggregation-induced emission (AIE) effect and an ability to assemble themselves into AIE polymer nanoparticles (NPs) during precipitation in a water/tetrahydrofuran (THF) mixture. The NPs also exhibit good dispersibility, stability, and biocompatibility. The AIE polymer NPs are used in imaging studies of HeLa cells.

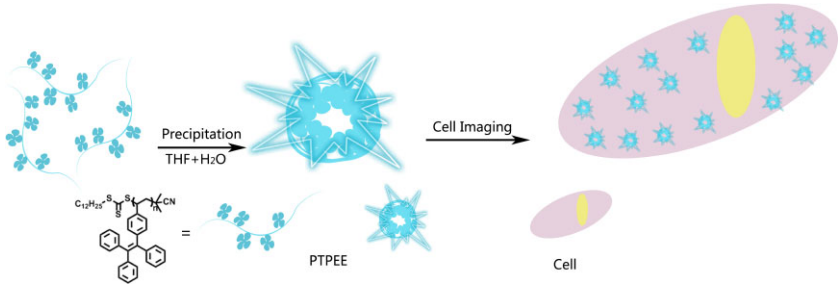

1. Introduction

Fluorescent probes have emerged as important techniques for cellular imaging to understand biochemical dynamics and monitor the biological structures as well as drug delivery over the past few decades.[1–8] Polymer luminophores, which combine the advantages of inorganic quantum dots (QDs) and organic dyes, are promising for bioimaging with excellent photostability, low cytotoxicity, and long-term cell tracking.[9–12] Obstacle of polymer luminophores in bioimaging applications is to render them dispersible in water with high fluorescence.[13] To achieve high dispersibility, extensive research efforts have been made and water-soluble polyelectrolytes as well as polymer-based nanoparticles (NPs) were investigated recently.[14,15] For polyelectrolytes, the synthesis generally requires sophisticated modification with introducing hydrophilic or ionic side chains to the polymer structures, which is time-consuming and largely increases the cost.[14] Moreover, most of these modifications may affect the intracellular physiology and usually lower the fluorescence quantum efficiencies of the polymer luminophores, because their excited states are quenched in water.

As compared to the synthesis of polyelectrolytes, preparation of polymer NPs serves as a simple and more general strategy. Actually, such polymer NPs can be formed facilely by method of self-assembly or nanoprecipitation with controlled sizes ranging from a few nanometers to

Dr. C. P. Ma, S. D. Xu, H. N. Zhu, Prof. Z. G. Chi, Dr. S. W. Liu, Prof. Y. Zhang, Prof. J. R. Xu
PCFM Lab, DSAPM Lab, KLGHEI of Environment and Energy Chemistry, State Key Laboratory of Optoelectronic Materials and Technologies, School of Chemistry and Chemical Engineering, Sun Yat-sen University, Guangzhou 510275, China
E-mail: chizhg@mail.sysu.edu.cn; xjr@mail.sysu.edu.cn
Q. Q. Ling, Prof. G. Zhang, Dr. X. Zhou
School of Pharmaceutical Sciences, Sun Yatsen University, Guangzhou 510275, China
E-mail: zhangge@mail.sysu.edu.cn

[a]**Supporting Information** is available from the Wiley Online Library or from the author

DOI: 10.1002/mabi.201300259

hundreds of nanometers.[8,15] However, most of these polymer luminophores have a common problem, that is, their fluorescence efficiencies dramatically decrease when they aggregate as NPs because of the strong intermolecular π–π stacking interactions of π-conjugated systems in the polymer chains and other non-radiative pathways.[16–19] This photophysical phenomenon is commonly known as aggregation-caused quenching (ACQ).[20,21]

In 2001, Tang and co-workers[22] reported some anti-ACQ compounds having aggregation-induced emission (AIE) characteristics. These luminogens are non-emissive in dilute solutions, but are induced to exhibit strong fluorescence in the aggregated or solid states which is totally opposite to the ACQ effect. Since then, AIE materials, with tetraphenylethene (TPE) core being a typical example, have attracted considerable research attention for their potential applications in various fields.[23–34] Hence, a satisfactory strategy for developing of high-performance fluorescent probes is to combine the advantages of AIE effect and polymer NPs. Although a lot of AIE-based organic dyes have been reported in recent years, polymer NPs with AIE properties are still very limited and remain seldom to be used in bioimaging.[12,35–43] The possible reason is that most of the AIE polymers cannot be prepared in a monodispersing form, and size and shape of the NPs are not appropriate for being uptaken by cells.[44,45] Therefore, we expect that fabrication of uniform polymer nanospheres with AIE activity can offer a novel fluorescent probe with an exceptional feature and promising application in bioimaging (Scheme 1).

2. Experimental Section

2.1. Materials and Measurements

(2-Bromoethene-1,1,2-triyl)tribenzene (P_3Br), (4-vinylphenyl) boronic acid, tetrabutylammonium tribromide (TBAB), tetrakis-(triphenylphosphine)palladium [$Pd(PPh_3)_4$], and potassium carbonate (K_2CO_3) purchased from Alfa Aesar were used as received. 2-Cyanopropan-2-yl dodecyl carbonotrithioate (CPTC) was purchased from Strem Chemicals. 2,2-Azobis(isobutyronitrile) (AIBN) was purchased from J&K Scientific Ltd. (China) and purified by recrystallization from ethanol and dried under vacuum. All other reagents and solvents were purchased as analytical grade from Guangzhou Dongzheng Company (China) and used without further purification. Dioxane was distilled from sodium/benzophenone. Ultra-pure water (18 MΩ cm) was used in the experiments.

Proton and carbon nuclear magnetic resonance (^1H NMR and ^{13}C NMR) spectra were measured on a Mercury-Plus 300 spectrometer [$CDCl_3$, tetramethylsilane (TMS) as the internal standard]. Mass spectra (MS) were measured on a Thermo DSQ MS spectrometer (ionization method: EI). Photoluminescence spectra (PL) were measured on a Shimadzu RF-5301pc spectrometer with a slit width (both excitation and emission) of 5 nm for the solution of the monomer and 1.5 nm for the solution of the polymers, respectively. Gel permeation chromatography (GPC) characterization was performed on a Waters Breeze at 25 °C with THF as the eluent against polystyrene standards. Scanning electron microscopy (SEM) images were obtained on a Hitachi S4800 microscope operated at 15 kV. Dynamic light scattering (DLS) measurements were conducted at 25 °C on a Brookhaven BI-200SM apparatus with a BI-9000AT digital correlator and a He–Ne laser at 532 nm. Transmission electron microscopy (TEM) observation was performed on a JEM-2010HR system. Zeta-potential measurements were made with a 90 Plus/BI-MAS equipment (Brookhaven Instruments Corporation, USA), and a standard electrophoresis mini-cell from Brookhaven was used. For the cell imaging, a fluorescent microscope (Nikon Eclipse Ti-S, Japan) with C-FL UV-2E/C DAPI filter cube (EX340-380/DM 400/BA435-485) and a confocal laser scanning microscopy (CLSM, Zeiss LSM710, Germany) with excitation wavelength of 405 nm were used.

2.2. Synthesis of 1,1,2,2-Tetraphenylethene (TPEE)

As shown in Scheme 2, P_3Br (2.00 g, 5.97 mmol) and 4-formylphenylboronic acid (1.06 g, 7.16 mmol) were dissolved in toluene (50 mL), TBAB (0.16 g) and 2 M potassium carbonate aqueous solution (12 mL). The mixture was stirred at room temperature for 0.5 h under argon gas followed adding $Pd(PPh_3)_4$ (0.005 g) and then heated to 85 °C for 24 h. After cooling, the product was extracted with dichloromethane–water. The organic layers were

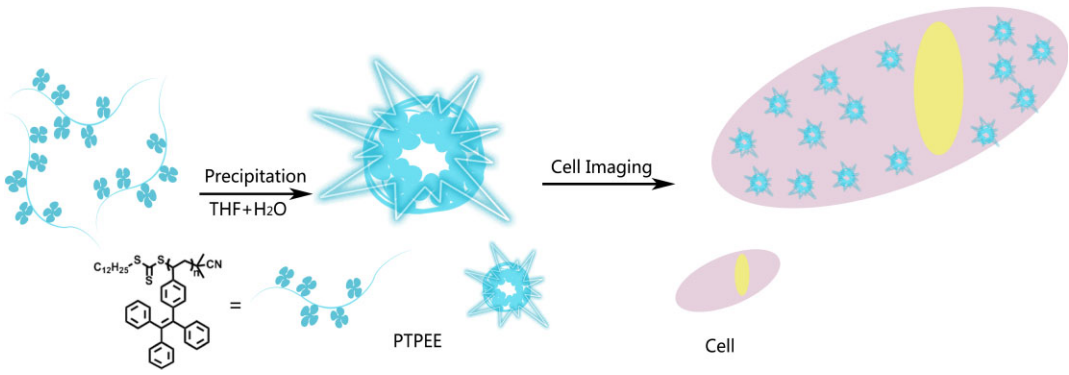

Scheme 1. Schematic showing preparation of **PTPEE** homopolymer fluorescent NPs and their use as cell imaging probes.

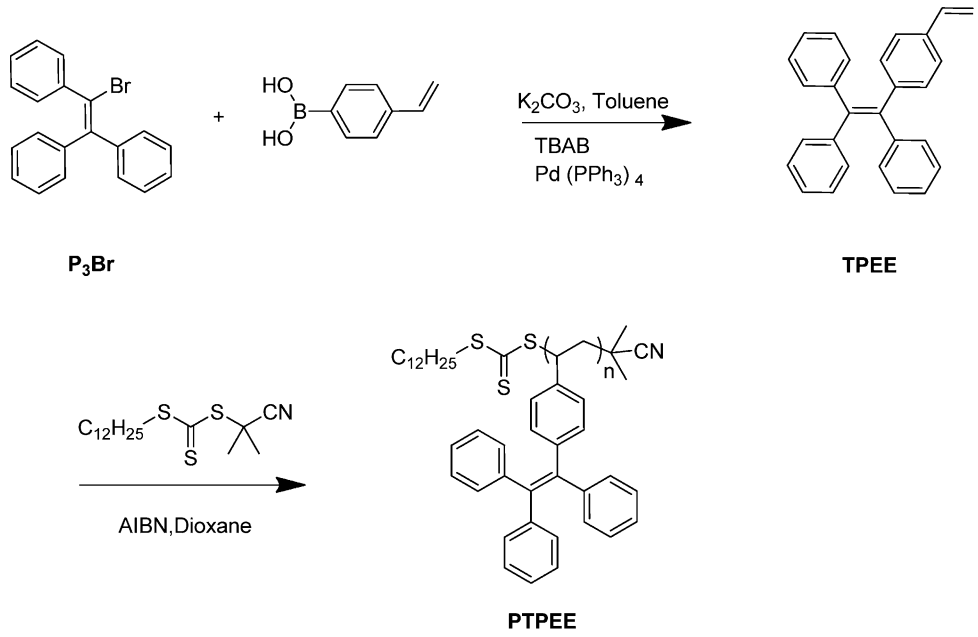

Scheme 2. Synthesis of monomer 1,1,2,2-tetraphenylethene (**TPEE**) and its homopolymers.

collected and dried under anhydrous sodium sulfate. The concentrated product was chromatographed on a silica gel column with *n*-hexane/CH_2Cl_2 (5:1 by volume) as eluent to give **TPEE** (1.60 g, yield 90.0%). ^{1}H NMR (300 MHz, $CDCl_3$): δ(ppm) = 5.20 (dd, 1 H, J = 0.73 Hz, 10.90 Hz), 5.68 (dd, 1 H, J = 0.80 Hz, 17.57 Hz), 6.63 (dd, 1 H, J = 10.87 Hz, 17.57 Hz), 6.96–7.20 (m, 19 H); ^{13}C NMR (75 MHz, $CDCl_3$): δ(ppm) = 143.87, 143.53, 141.22, 140.75, 136.77, 135.70, 131.56, 127.82, 126.66, 125.74, 113.68; MS (EI), m/z: 358 (calcd. for $C_{28}H_{22}$ 358).

2.3. Synthesis of Poly[(2-(4-vinylphenyl)ethene-1,1,2-triyl)tribenzene] (PTPEE10, 20, 40, and 80)

The **PTPEE** polymers were synthesized following the route shown in Scheme 2. For the synthesis of **PTPEE10**, **TPEE** (0.358 g, 1.0 mmol), CPTC (34.6 mg, 0.10 mmol), and AIBN (3.28 mg, 0.02 mmol) were dissolved in 2 mL of dioxane. The solution was degassed three times through a standard freeze–thaw process. The monomers were polymerized at 75 °C for 24 h under argon. Homopolymer was precipitated into 100 mL of *n*-hexane from the dioxane solution twice, resulting in 315 mg of **PTPEE10** as pale yellow powder (yield 88.0%). 326 mg of **PTPEE20**, 340 mg of **PTPEE40** and 329 mg of **PTPEE80** were obtained by using similar protocols except the amounts of CPTC used were 17.3, 8.64, and 4.32 mg, and AIBN used were 1.64, 0.82, and 0.41 mg for preparing **PTPEE20**, **PTPEE40**, and **PTPEE80**, respectively. ^{1}H NMR for all the **PTPEE** polymers (300 MHz, $CDCl_3$): δ(ppm) = 6.10–7.20 (broad, aromatic protons), 5.30 (CH_2Cl_2 remained), 1.00–2.50 (broad, –CH_2– and –CH (C_6H_4) CH_2–), 0.95–0.98 (–CH_3).

2.4. Quantum Efficiency Measurements

Fluorescence quantum yields for the **PTPEE** polymers were obtained by comparing the integrated fluorescence spectra and absorbance spectra of the polymers in solutions to the fluorescence spectrum and absorbance spectrum of quinine sulfate in 1.0 N H_2SO_4 (Φ = 0.55, excitation wavelength of 350 nm) with a correction of refractive index differences using:

$$\eta_s = \eta_r \left(\frac{A_r}{A_s}\right)\left(\frac{I_s}{I_r}\right)\left(\frac{n_s^2}{n_r^2}\right) \quad (1)$$

where (η_s) and (η_r) are the fluorescence quantum yield of the samples (**PTPEE** polymers) and the standard, respectively. A_s and A_r are the absorbance of the samples and the standard at the excitation wavelength, respectively. I_s and I_r are the integrated emission intensities of the samples and the standard. n_s and n_r are the refractive indices of the corresponding solvents of the solutions, respectively (the refractive indices of H_2O and THF are 1.333 and 1.407, respectively).

2.5. Preparation of PTPEE40 NPs

The preparation of **PTPEE40** NPs was carried out as follows. **PTPEE40** (10 mg) was dissolved in 10 mL of THF overnight. The solution was then filtered through a 0.2 μm filter. 1 mL of the **PTPEE40**/THF solution was added quickly to 9 mL of deionized water while the mixture was sonicated.

2.6. Cell Culture

HeLa cells (a human cervical carcinoma cell line) were maintained in RPMI 1640 (Invitrogen) supplemented with 10% heat-inactivated endotoxin-free newborn calf serum (HyClone), under a humidified 5% CO_2 atmosphere at 37 °C in an incubator.

2.7. Cytotoxicity of PTPEE40 NPs

The cell viability of **PTPEE** NPs on HeLa cells was evaluated by thiazolyl blue tetrazolium bromide (MTT) assay. Briefly, HeLa cells seeded into 96-well plates at a density of 5×10^4 cells mL^{-1} and were cultured for 24 h. Then, the cells were incubated with 0, 3.13, 6.25, 12.5, 25.0, 50.0 $\mu g\ mL^{-1}$ **PTPEE** NPs for 24 h. After removing the culture medium, 10 μL of 5 $\mu g\ mL^{-1}$ MTT was added to each well and incubated for 3.5 h, then, 200 μL DMSO solvent was added to and the absorbance was read at 488 nm with a reference filter of 620 nm by iMark Microplate Absorbance Reader (Bio-Rad, USA).

Cell morphology was also observed to examine the effect of **PTPEE** NPs to HeLa cells. Briefly, cells were seeded into 6-well plated at a density of 1×10^4 cells mL^{-1} and then were cultured for 24 h. After removal of old culture media, the cells were incubated with 0, 3.13, 6.25, 12.5, 25.0, $\mu g\ mL^{-1}$ **PTPEE40** for 24 h, respectively. The morphology of cells was observed with an optical microscopy (Zeiss, Germany).

2.8. Cell Imaging Using PTPEE40 NPs

Cells were grown on 6-well plates and 2 mm confocal culture dish, respectively. After 12 h of cultivation, cells were cultured with 6.25 $\mu g\ mL^{-1}$ **PTPEE40** NPs [Containing 0.625% (volume fraction) THF, which do not influence on the cell activity[46]] for 12 h. Cells were washed with phosphate buffered saline (PBS) for four times. Samples were examined with the fluorescent microscope and the CLSM to analyze the translocation of **PTPEE40** NPs.

3. Results and Discussion

The **PTPEE** polymers were synthesized following the route shown in Scheme 2. The monomer (2-(4-vinylphenyl) ethene-1,1,2-triyl)tribenzene (**TPEE**) was synthesized by the Suzuki reaction. CPTC was used as a RAFT reagent to control the RAFT polymerization of **TPEE** in the presence of the initiator, azodiisobutyronitrile (AIBN). The data about **PTPEE** homopolymers obtained at different CPTC proportion of RAFT polymerization are summarized in

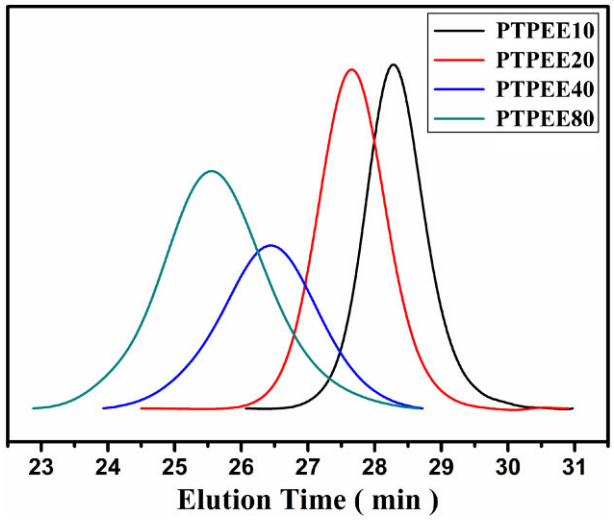

Figure 1. GPC traces of **PTPEE** homopolymers obtained with different CPTC concentrations.

Table 1. The molecular weight of the homopolymers increased with decreased CPTC proportion, and the molecular weight distribution remained relatively narrow ($\overline{M}_w/\overline{M}_n = 1.13$–$1.32$). As shown in Figure 1, the GPC traces of the **PTPEE** homopolymers shifted toward higher values along the molar mass scale with decreased CPTC proportion, and appeared monomodal and relatively symmetric in shape.[47] By controlling the CPTC proportion, homopolymers with different molecular weights and narrow distributions can be obtained.

Table 1 also showed that the polydispersity index (PDI) increased with decreased CPTC proportion, and the conversion of **TPEE** to polymers did not exceed 60%. This behavior is similar to that already observed in the case of styrene and benzyldiethoxyphosphoryldithioformate.[48–50] Compared with the monomer conversion rate, the rate constant of radical formation was not

Table 1. Results for the synthesis of **PTPEE** homopolymers.

Sample	PTPEE10	PTPEE20	PTPEE40	PTPEE80
$\overline{M}_n$(GPC)[a)]	2 085	3 304	7 325	11 701
$\overline{M}_n$(NMR)[b)]	2 494	2 852	5 358	12 047
PDI[a)]	1.13	1.14	1.26	1.32
$\overline{DP}$[a)]	6	9	20	33
[TPEE]/[CPTC]	10:1	20:1	40:1	80:1
Conv. [%][a)]	60%	45%	50%	41%

[a)]PDI, polydispersity index; $\overline{DP}$, polymerization degree; both determined by GPC; [b)]determined by ^1H NMR with $CDCl_3$ as solvent. Polymerization time 24 h.

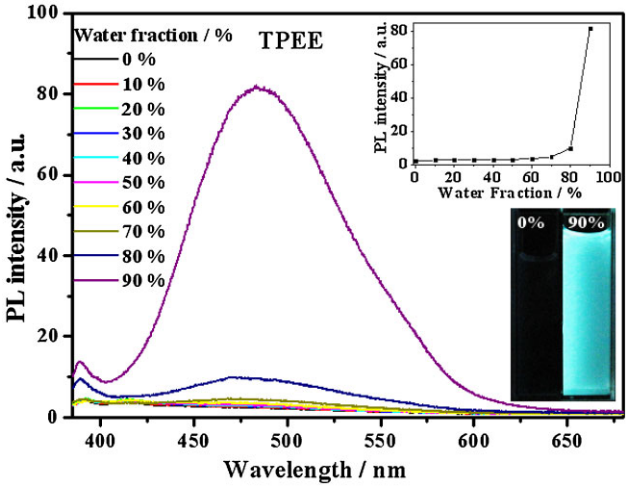

Figure 2. PL spectra of the dilute solutions of monomer **TPEE** in water/THF mixtures with different water fractions (concentration: 10^{-5} M; excitation wavelength: 350 nm). The insets depict the changes in PL peak intensity (up) and emission images of the compound in pure THF and 90% water fraction mixtures under 365 nm UV illumination (down).

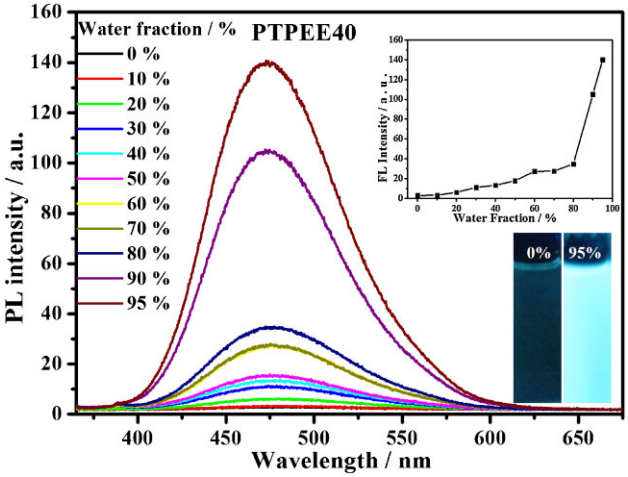

Figure 3. PL spectra of the dilute solutions of **PTPEE40** homopolymer in H_2O/THF mixture with different water fractions (concentration: 0.1 mg mL^{-1}; excitation wavelength: 350 nm). The insets depict the changes in PL peak intensity (up) and emission images of the compound in pure THF and 95% water fraction mixtures under 365 nm UV illumination (down).

sufficiently high. The initiating activity of the polymer chain may have been inhibited because of the steric effects of the pendant group TPE, resulting in the occurrence of a coupling reaction during polymerization.

TPEE and all four obtained **PTPEE** samples display AIE behaviors in H_2O/THF mixed solutions. The intensity of emission of the **TPEE** was enhanced with increased water content up to 90% (Figure 2). And much more obvious AIE behaviors were observed when the **TPEE** was replaced by the four **PTPEE** samples. For example, **PTPEE40** exhibited nearly no emission at 470 nm in THF solution. However, the addition of 90% water to THF solution enhanced the emission intensity up to 100-fold (Figure 3), showing a significant AIE effect. Further evidence was obtained by quantum efficiency measurement, as shown in Figure S8 of Supporting Information, the quantum efficiencies of the **PTPEE** samples in H_2O/THF were increased by increasing the water content, as hydrophobic TPE segments aggregate together and restrict the intramolecular rotations of the fluorophores, increasing the fluorescence quantum efficiencies.[43] In addition, at the same H_2O/THF fraction, the polymers with higher molecular weight exhibit higher quantum efficiencies, due to the increase of hydrophoby.

Figure 4A shows the SEM image of the aggregation morphologies of **PTPEE40** when the water content was up to 90%. The SEM images show the formation of spherical particles "dimpled beads",[51] separated from one another with dimples on their smooth surfaces, with the sizes varying from 400 to 800 nm. Interestingly, only one "dimple" was observed on each particle. These morphologies were also confirmed by the TEM images in Figure 4C. However, the monomer cannot form regularly shaped particles, as shown in Figure S9 in the Supporting Information, and precipitation was formed in the solutions of **TPEE** within 24 h.

The sizes of **PTPEE** spherical particles can be controlled by the speed and sequence of adding the THF solution of **PTPEE** into the water. For **PTPEE40**, the "dimpled beads" with a diameter of above 400 nm were observed when the dropping speed of water was slow. By contrast, NPs with a diameter of 100–150 nm were obtained when 1 mL of THF solution of **PTPEE** was quickly charged into 9 mL of deionized water, as shown in Figure 4,D. The method for the rapid addition of polymer solution into an excess volume of water is simply "precipitation".[15] In the present study, the preparation process did not involve any surfactant and could be further applied to a series of polymers, and thus this method is simple and easy to prepare AIE NPs. The emission λ_{max} of the "dimpled beads" appeared at a wavelength of only 5 nm (475 nm vs 470 nm) longer than that of the NPs, and had a more intense emission (Figure 5). The diameter of the **PTPEE10** NPs was the smallest among the four polymers (**PTPEE10**, 167 nm; **PTPEE20**, 197 nm; **PTPEE40**, 192 nm; **PTPEE80**, 204 nm), as shown in Table 2. It could be deduced from these data that the diameter may have no direct obvious influence on the molecular weight of the homopolymers. The diameters of the NPs based on SEM and TEM images were smaller than those measured by DLS. The NPs were stable in solution, as the intensity of emission of the solutions of NPs almost kept

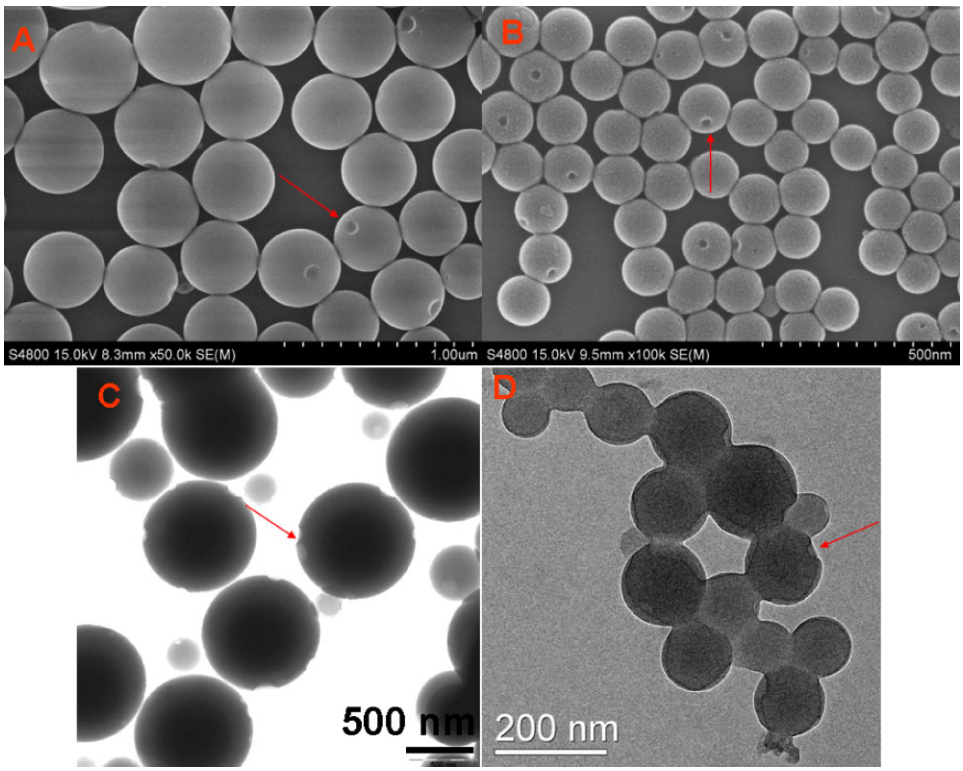

Figure 4. A,B) SEM images and C,D) TEM images of **PTPEE40** particles. A,C) Particles obtained when the 9 mL deionized water was slowly added into the 1 mL THF solution of **PTPEE40** homopolymer; B,D) NPs obtained when 1 mL THF solution of **PTPEE40** was added quickly to 9 mL deionized water (concentration: 0.1 mg mL^{-1}).

constant within 48 h, as shown in Figure S10 (Supporting Information), and there was no precipitation of the particles from the solutions within a week. The stability of the NPs was also demonstrated by Zeta potentials of the **PTPEE40** and **PTPEE80** NPs, which ranged from −30 to −20 mV. As we known, the surface potential is considered to be the main reason for the stability of homopolymer NPs, and may originate from the selective adsorption of OH^- anions from ionized water.[52] Thus, these AIE NPs were stable under the experimental conditions.

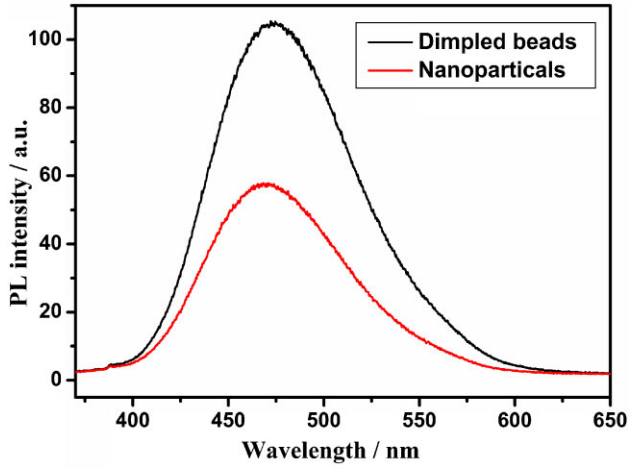

Figure 5. PL spectra of the dimpled beads (9 mL deionized water was slowly added into the 1 mL homopolymer THF solution) and NPs (1 mL homopolymer THF solution was added quickly to 9 mL deionized water) (concentration: 0.1 mg mL^{-1}; excitation wavelength: 350 nm).

The biocompatibility of the **PTPEE** NPs was subsequently evaluated.[53] Figure 6A–C showed the morphologies of HeLa cells incubated with different **PTPEE** concentrations (0, 6.25, and 25.0 μg mL^{-1}) for 24 h. The HeLa cells did not show any obvious morphological changes. For **PTPEE20**/**PTPEE40**/**PTPEE80** NPs, cell viability of the MTT assay (Figure 6D) revealed no significant cytotoxic effect at the concentration of up to 25 μg mL^{-1}. And the relatively high cytotoxicity of **PTPEE10** may be due to the excess intracellular accumulation of **PTPEE10**, because the NP diameter of **PTPEE10** is smaller than the other three polymers, as shown in Table 2, so it is easier for the NP of **PTPEE10** to be internalized into cells. Nevertheless, both the cell morphological observation and cell viability examination suggest that the **PTPEE** NPs were biocompatible with HeLa cells, which should be valuable for their further biological imaging applications.

To investigate the potential biomedical applications of **PTPEE** NPs, they were used as probes for cell imaging under

Table 2. Physical parameters of **PTPEE** homopolymer NPs with different molecule weight[a)]

System	PTPEE10	PTPEE20	PTPEE40	PTPEE80
R_{DLS} [nm]	167.0	197.3	191.2	203.6
PDI	0.168	0.027	0.186	0.053
ξ-potential [mV]	-11.09 ± 1.45	-14.64 ± 1.51	-21.73 ± 2.88	-24.49 ± 0.86

[a)] R_{DLS} is the particle diameter determined by DLS; PDI and ξ-potential are the polydispersity index and zeta potential of NPs, respectively.

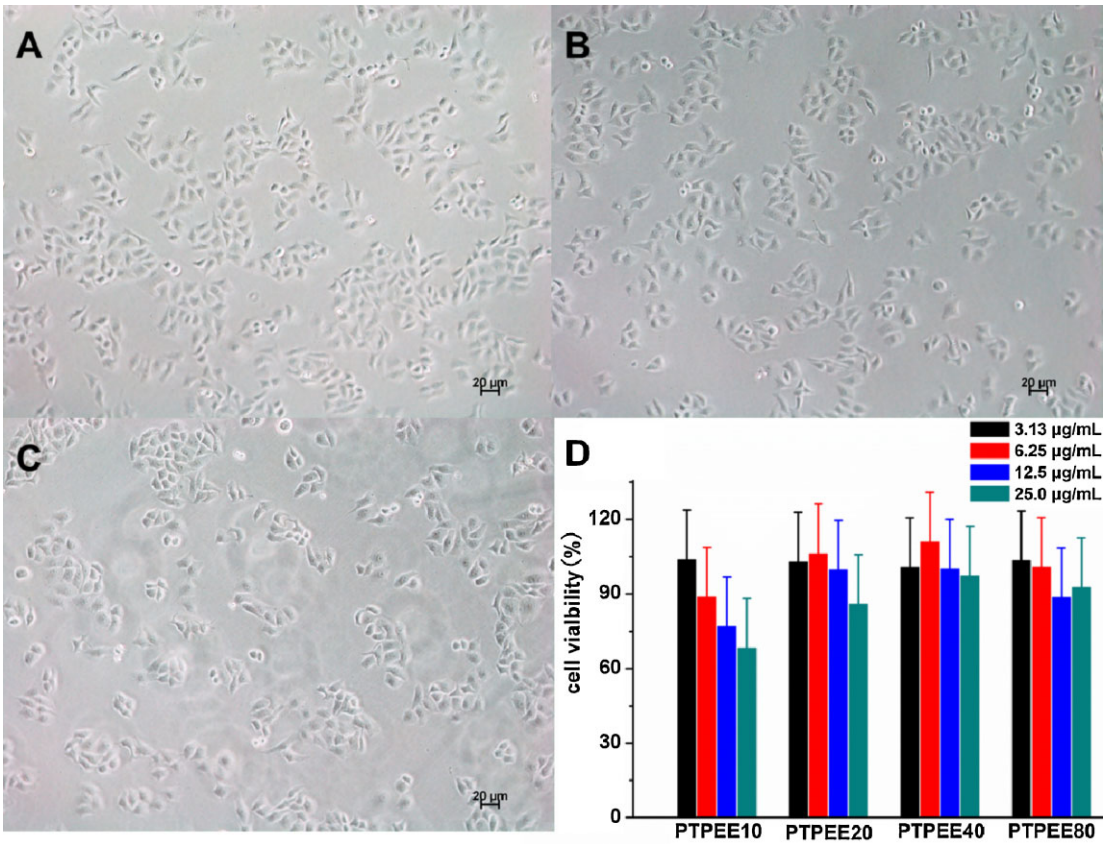

Figure 6. Biocompatibility of **PTPEE** NPs: optical microscopy photos of HeLa cells incubated with different concentrations of **PTPEE40** NPs A) 0 μg mL^{-1}, B) 6.25 μg mL^{-1}, C) 25.0 μg mL^{-1} (scale bars: 20 μm); D) concentration-dependent cytotoxicity of **PTPEE** NPs.

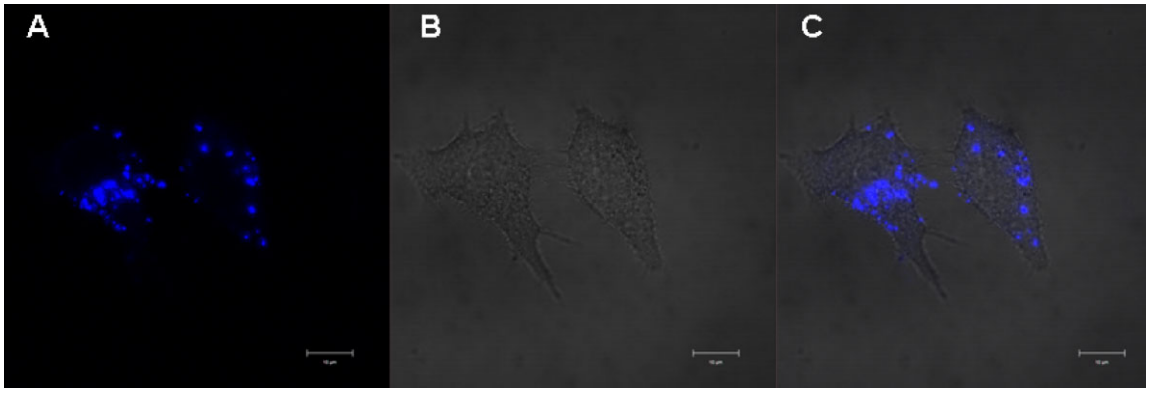

Figure 7. CLSM images of HeLa cells stained by **PTPEE40** NPs. A) 405 nm excitation, B) bright field, C) overlay of image (A,B) (scale bars: 10 μm).

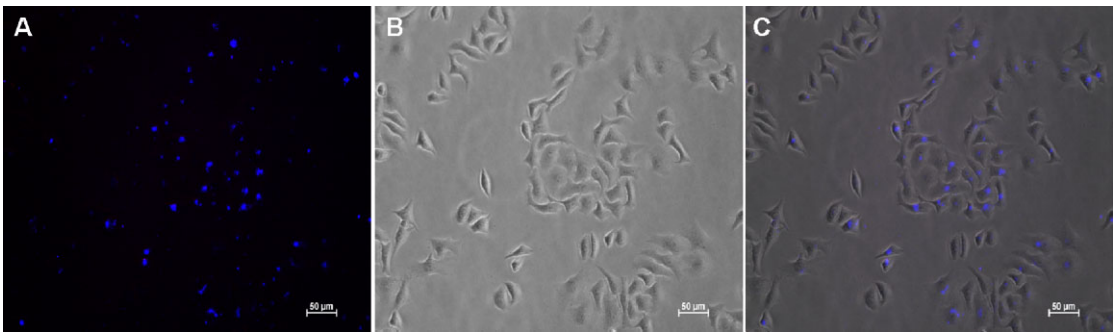

Figure 8. Fluorescence images of HeLa cells stained by **PTPEE40** NPs. A) 405 nm excitations, B) bright field, C) overlay of image (A,B) (scale bar: 50 μm).

CLSM. As shown in Figure 7, blue fluorescence was observed when the cells were incubated with 6.25 $\mu g \cdot mL^{-1}$ **PTPEE40** NPs for 12 h. Blue fluorescence areas were found within the HeLa cells, specifically, the cytoplasm, suggesting that the **PTPEE** NPs were easily internalized into cells. The mechanism of the cellular uptake of the particles should be macropinocytosis, because cells can internalize particles with diameter larger than 150 nm through this pathway.[54,55] on the other hand, strongly negatively charged polymers prefer macropinocytosis pathway to be internalized into cells.[56] Notably, **PTPEE40** with a low concentration (6.25 $\mu g\ mL^{-1}$) led to clearer cell imaging not only under CLSM, but also under fluorescence microscopy (Figure 8), suggesting that the **PTPEE** NPs had potential biological imaging applications.

4. Conclusion

A series of new homopolymers with various degrees of polymerization, i.e., poly[(2-(4-vinylphenyl)ethene-1,1,2-triyl) tribenzene] homopolymers, were successfully synthesized by RAFT polymerization. The homopolymers exhibited a significant AIE effect with 100-fold increase in emission intensity from solution to nanosuspension. The homopolymers can assemble themselves to AIE NPs by quickly charging THF solution into deionized water. The NPs exhibited good dispersibility, stability and biocompatibility. The current study provides a new framework to fabricate more stable surfactant-free AIE polymer NPs. The NPs were then used for imaging studies of HeLa cells and were found to have potential biomedical applications. A comprehensive study on the RAFT polymerization of **TPEE** monomer, assembly mechanism and further work in this respect are now in progress.

Acknowledgements: C.P.M. and Q.Q.L. contributed equally to this work. This work was supported by the National Natural Science Foundation of China (51173210 and 51073177), the Fundamental Research Funds for the Central Universities and Natural Science Foundation of Guangdong (S2011020001190).

Received: May 27, 2013; Revised: August 11, 2013; Published online: September 17, 2013; DOI: 10.1002/mabi.201300259

Keywords: aggregation-induced emission; cell imaging; nanoparticles; RAFT polymerization

[1] L. D. Tennyson, B. Clemens, *Chem. Soc. Rev.* **2012**, *41*, 2885.
[2] D. R. Cooper, J. L. Nadeau, *Nanoscale* **2009**, *1*, 183.
[3] X. Feng, L. Liu, S. Wang, D. Zhu, *Chem. Soc. Rev.* **2010**, *39*, 2411.
[4] J. Kim, Y. Piao, T. Hyeon, *Chem. Soc. Rev.* **2009**, *38*, 372.
[5] A. M. Koch, F. Reynolds, M. F. Kircher, H. P. Merkle, R. Weissleder, L. Josephson, *Bioconjugate Chem.* **2003**, *14*, 1115.
[6] J. Chan, S. C. Dodani, C. J. Chang, *Nat. Chem.* **2012**, *4*, 973.
[7] J. Zhang, R. E. Campbell, A. Y. Ting, R. Y. Tsien, *Nat. Rev. Mol. Cell Biol.* **2002**, *3*, 906.
[8] Z. Y. Tian, J. B. Yu, C. F. Wu, C. Szymanski, J. McNeill, *Nanoscale* **2010**, *2*, 1999.
[9] D. Tuncel, H. V. Demir, *Nanoscale* **2010**, *2*, 484.
[10] K. Y. Pu, B. Liu, *Adv. Funct. Mater.* **2011**, *21*, 3408.
[11] A. Kaeser, A. Schenning, *Adv. Mater.* **2010**, *22*, 2985.
[12] M. Li, Y. Hong, Z. Wang, S. Chen, M. Gao, R. T. K. Kwok, W. Qin, J. W. Y. Lam, Q. Zheng, B. Z. Tang, *Macromol. Rapid Commun.* **2013**, *34*, 767.
[13] K. Li, B. Liu, *J. Mater. Chem.* **2012**, *22*, 1257.
[14] A. Duarte, K. Y. Pu, B. Liu, G. C. Bazan, *Chem. Mater.* **2011**, *23*, 501.
[15] J. Pecher, S. Mecking, *Chem. Rev.* **2010**, *110*, 6260.
[16] A. J. Qin, J. W. Y. Lam, L. Tang, C. K. W. Jim, H. Zhao, J. Z. Sun, B. Z. Tang, *Macromolecules* **2009**, *42*, 1421.
[17] A. J. Qin, C. K. W. Jim, Y. H. Tang, J. W. Y. Lam, J. Z. Liu, F. Mahtab, P. Gao, B. Z. Tang, *J. Phys. Chem. B* **2008**, *112*, 9281.
[18] W. Z. Yuan, A. J. Qin, J. W. Y. Lam, J. Z. Sun, Y. Q. Dong, M. Haussler, J. Z. Liu, H. P. Xu, Q. Zheng, B. Z. Tang, *Macromolecules* **2007**, *40*, 3159.
[19] A. Wakamiya, K. Mori, S. Yamaguchi, *Angew. Chem., Int. Ed.* **2007**, *46*, 4273.
[20] R. Jakubiak, C. J. Collison, W. C. Wan, L. J. Rothberg, B. R. Hsieh, *J. Phys. Chem. A* **1999**, *103*, 2394.

[21] S. W. Thomas, G. D. Joly, T. M. Swager, *Chem. Rev.* **2007**, *107*, 1339.
[22] J. D. Luo, Z. L. Xie, J. W. Y. Lam, L. Cheng, H. Y. Chen, C. F. Qiu, H. S. Kwok, X. W. Zhan, Y. Q. Liu, D. B. Zhu, B. Z. Tang, *Chem. Commun.* **2001**, 1740.
[23] C. Chen, J.-Y. Liao, Z. Chi, B. Xu, X. Zhang, D.-B. Kuang, Y. Zhang, S. Liu, J. Xu, *J. Mater. Chem.* **2012**, *22*, 8994.
[24] Z. Chi, X. Zhang, B. Xu, X. Zhou, C. Ma, Y. Zhang, S. Liu, J. Xu, *Chem. Soc. Rev.* **2012**, *41*, 3878.
[25] Y. Hong, J. W. Y. Lam, B. Z. Tang, *Chem. Soc. Rev.* **2011**, *40*, 5361.
[26] H. Li, Z. Chi, X. Zhang, B. Xu, S. Liu, Y. Zhang, J. Xu, *Chem. Commun.* **2011**, *47*, 11273.
[27] A. Qin, J. W. Y. Lam, B. Z. Tang, *Prog. Polym. Sci.* **2012**, *37*, 182.
[28] H. Shi, R. T. K. Kwok, J. Liu, B. Xing, B. Z. Tang, B. Liu, *J. Am. Chem. Soc.* **2012**, *134*, 17972.
[29] H. Shi, J. Liu, J. Geng, B. Z. Tang, B. Liu, *J. Am. Chem. Soc.* **2012**, *134*, 9569.
[30] M. Wang, G. Zhang, D. Zhang, D. Zhu, B. Z. Tang, *J. Mater. Chem.* **2010**, *20*, 1858.
[31] B. Xu, M. Xie, J. He, B. Xu, Z. Chi, W. Tian, L. Jiang, F. Zhao, S. Liu, Y. Zhang, Z. Xu, J. Xu, *Chem. Commun.* **2013**, *49*, 273.
[32] Z. Yang, Z. Chi, T. Yu, X. Zhang, M. Chen, B. Xu, S. Liu, Y. Zhang, J. Xu, *J. Mater. Chem.* **2009**, *19*, 5541.
[33] X. Zhang, Z. Chi, B. Xu, L. Jiang, X. Zhou, Y. Zhang, S. Liu, J. Xu, *Chem. Commun.* **2012**, *48*, 10895.
[34] J. Liu, J. W. Y. Lam, B. Z. Tang, *J. Inorg. Organomet. Polym.* **2009**, *19*, 249.
[35] B. Xu, Z. Chi, Z. Yang, J. Chen, S. Deng, H. Li, X. Li, Y. Zhang, N. Xu, J. Xu, *J. Mater. Chem.* **2010**, *20*, 4135.
[36] W. Z. Yuan, P. Lu, S. M. Chen, J. W. Y. Lam, Z. M. Wang, Y. Liu, H. S. Kwok, Y. G. Ma, B. Z. Tang, *Adv. Mater.* **2010**, *22*, 2159.
[37] S. Kim, Q. Zheng, G. S. He, D. J. Bharali, H. E. Pudavar, A. Baev, P. N. Prasad, *Adv. Funct. Mater.* **2006**, *16*, 2317.
[38] Z. Chang, Y. Jiang, B. He, J. Chen, Z. Yang, P. Lu, H. S. Kwok, Z. Zhao, H. Qiu, B. Z. Tang, *Chem. Commun.* **2013**, *49*, 594.
[39] B. Xu, Z. Chi, J. Zhang, X. Zhang, H. Li, X. Li, S. Liu, Y. Zhang, J. Xu, *Chem. Asian J.* **2011**, *6*, 1470.
[40] H. Tong, Y. N. Hong, Y. Q. Dong, M. Haussler, J. W. Y. Lam, Z. Li, Z. F. Guo, Z. H. Guo, B. Z. Tang, *Chem. Commun.* **2006**, 3705.
[41] B. Xu, Z. Chi, H. Li, X. Zhang, X. Li, S. Liu, Y. Zhang, J. Xu, *J. Phys. Chem. C* **2011**, *115*, 17574.
[42] X. Luo, W. Zhao, J. Shi, C. Li, Z. Liu, Z. Bo, Y. Q. Dong, B. Z. Tang, *J. Phys. Chem. C* **2012**, *116*, 21967.
[43] H. G. Lu, F. Y. Su, Q. Mei, X. F. Zhou, Y. Q. Tian, W. J. Tian, R. H. Johnson, D. R. Meldrum, *J. Polym. Sci. Polym. Chem.* **2012**, *50*, 890.
[44] P. Decuzzi, B. Godin, T. Tanaka, S. Y. Lee, C. Chiappini, X. Liu, M. Ferrari, *J. Controlled Release* **2010**, *141*, 320.
[45] A. Albanese, P. S. Tang, W. C. W. Chan, *Annu. Rev. Biomed. Eng.* **2012**, *14*, 1.
[46] C. Boesch-Saadatmandi, G. Rimbach, A. Jungblut, J. Frank, *Cytotechnology* **2011**, *63*, 89.
[47] Y. Zhao, X. Shi, H. Gao, L. Zhang, F. Zhu, Q. Wu, *J. Mater. Chem.* **2012**, *22*, 5737.
[48] A. Alberti, M. Benaglia, M. Guerra, M. Gulea, P. Hapiot, M. Laus, D. Macciantelli, S. Masson, A. Postma, K. Sparnacci, *Macromolecules* **2005**, *38*, 7610.
[49] M. Laus, R. Papa, K. Sparnacci, A. Alberti, M. Benaglia, D. Macciantelli, *Macromolecules* **2001**, *34*, 7269.
[50] M. L. Coote, D. J. Henry, *Macromolecules* **2005**, *38*, 1415.
[51] J. Wang, M. Kuang, H. W. Duan, D. Y. Chen, M. Jiang, *Eur. Phys. J. E* **2004**, *15*, 211.
[52] S. M. Yang, D. Lu, L. L. Tian, F. He, G. Chen, F. Z. Shen, H. Xu, Y. G. Ma, *Nanoscale* **2011**, *3*, 2261.
[53] X. Zhang, S. Wang, C. Fu, L. Feng, Y. Ji, L. Tao, S. Li, Y. Wei, *Polym. Chem.* **2012**, *3*, 2716.
[54] S. E. A. Gratton, P. A. Ropp, P. D. Pohlhaus, J. C. Luft, V. J. Madden, M. E. Napier, J. M. DeSimone, *PNAS* **2008**, *105*, 11613.
[55] I. A. Khalil, K. Kogure, S. Futaki, S. Hama, H. Akita, M. Ueno, H. Kishida, M. Kudoh, Y. Mishina, K. Kataoka, M. Yamada, H. Harashima, *Gene Ther.* **2007**, *14*, 682.
[56] J. Liu, H. Bauer, J. Callahan, P. Kopečková, H. Pan, J. Kopeček, *J. Controlled Release* **2010**, *143*, 71.